ISSN 1392–1320 MATERIALS SCIENCE (MEDŽIAGOTYRA). Vol. 20, No. 1. 2014

Effect of Au Nanoparticles Doping on The Properties of TiO_2 Thin Films

Aytaç GÜLTEKİN *

Karamanoğlu Mehmetbey University, Faculty of Engineering, Department of Energy Systems Engineering, Karaman, Turkey

crossref http://dx.doi.org/10.5755/j01.ms.20.1.3709

Received 07 March 2013; accepted 10 November 2013

In this study, pure and gold (Au) nanoparticles doped TiO_2 thin films (Au/Ti = 10, 20, 30, 40 and 50 at%) were prepared by sol-gel method and the impact of Au nanoparticles doping on the optical, structural and morphological properties of these thin films was examined. All thin films were characterized using ultraviolet-visible-near infrared (UV-Vis-NIR) spectrophotometry, X-ray diffraction (XRD), transmission electron microscopy (TEM) and atomic force microscopy (AFM). The optical band gap of the thin films increases from 3.74 eV to 3.89 eV with the increase of Au nanoparticles concentrations due to the Moss-Burstein effect. XRD results show that all thin films have cubic poly-crystal structure and the intensities of peaks of the crystalline phase increased with the increase of Au nanoparticles concentrations. The AFM results indicate that the TiO_2 thin films are formed from the nanoparticles and the grain size of the films is changed with Au doping level. Consequently, it is shown that the structural, morphological and optical properties of the TiO_2 thin films could be changed by Au nanoparticles-doping.

Keywords: Au nanoparticles, TiO_2 thin films, optical, structural and morphological properties.

1. INTRODUCTION

Titanium dioxide (TiO_2) is a non-toxic and low cost material. Because of its peerless properties such as, high refractive index, high transparency in the visible range, high dielectric constant, ability to be easily doped with active ions, good chemical stability, it has potential applications, including LEDs, gas sensors, solar cells, heat reflectors, light transparent electrodes and thin film photovoltaic and many other opto-electronic devices [1 – 17].

The doping of TiO_2 with different metal ions has frequently been tried not only to retard the quick recombination of electron-hole pair, but also to increase the absorption of visible light by providing faulty states in the band gap [18]. Modification of the TiO_2 surface with metal ions has been successful used to enhance the optical and electrical activity of TiO_2 and thus, to improve quantum yield because of a raise in the rate of electron transfer to the oxidant [19].

Many researchers have recently been focused on examination of metal oxide thin films with metal nanoparticles such as Fe, Ni, Au, Ag, Cu deposited on oxide surfaces, embedded within porous network or encapsulated in its matrices since such materials have wide applications in diagnostics, catalysis and photocatalysis [20]. In doping of metal oxide thin films, metallic nanoparticles (NPs) can produce quenching or heightening of the magnitude of the optical absorptive nonlinearities [21]. Among of metallic NPs, Au nanoparticles have attracted much attention on potential applications due to their nonlinear optical properties, irresistible magnitude and quick response [22]. The plasmon resonance led to photo-excitation of Au nanoparticles and charge separation occur due to electron transfer from Au nanoparticles by photo-excitation to TiO_2 conduction band and simultaneous transfer of electrons from an appropriate/spesific donor in the solution to the Au nanoparticles [23].

*Corresponding author. Tel.: +90-338-226-5055; fax.: +90-338-226-2116.
E-mail address: *aysari@yahoo.com* (A. Gültekin)

The first goal of this study is to synthesize TiO_2 thin films and Au NPs by using sol-gel method and Brust method, respectively, and then, to prepare the various (i. e.; 10 %, 20 %, 30 %, 40 %, 50 at%) Au NPs doped TiO_2 thin films. The second goal of this study is to investigate the effects of Au NPs doping on optical, structural and morphological properties of these thin films.

2. EXPERIMENTAL PROCEDURE

Au nanoparticles were prepared by a chemical reduction of $HAuCl_4$ (pH ca. 7.8) ammoniacal aqueous solution with aqueous $NaBH_4$ solution that denominated as above-mentioned Brust method. [24 – 25]. A TEM (Transmission Electron Microscopy) image of Au nanoparticles using a FEITecnai^{TM} G^2 Sprit transmission electron microscope (20 kV – 120 kV) is given in Fig. 1. The shape of the nanoparticles is close to spherical, aggregated and with an average size of approximately 15 nm.

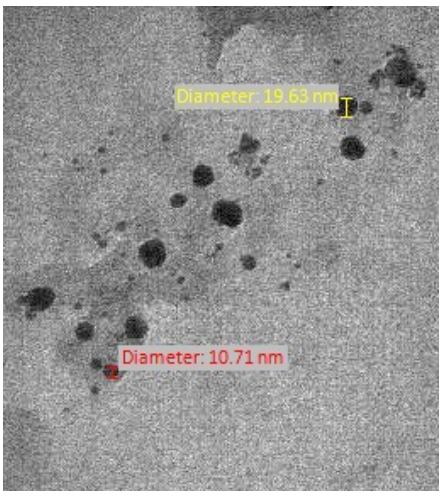

Fig. 1. A TEM image of Au NPs

In the typical preparation procedure of TiO_2 solution, first of all, 2.4 ml of titanium tetraisopropoxide [($Ti(OC_3H_7)_4$, Merck] was dissolved in 25 ml of ethyl

alcohol [C_2H_6O, Merck] and the solution stirring was continued for 1 h. After that period, 5 ml of glacial acetic acid [CH_3COOH, Merck] and 25 ml of ethyl alcohol were added in the solution and stirring was continued for 1 h. As the final step, 1.5 ml of triethylamine [$(C_2H_5)_3N$, Merck] was added in the solution, and the last solution was stirred with magnetic stirrer for 1 h. In order to synthesize Au nanoparticles doped TiO_2 solution, Au nanoparticles were added into the TiO_2 solution (Au/Ti (at%) = 1/10, 2/10, 3/10, 4/10, 5/10) and the solutions were stirred with a magnetic stirrer for two hours. Finally, pure and Au-doped TiO_2 solutions were kept at room temperature for one day before deposition.

Microscope glass slides were used as the substrates for thin films. Before deposition, the glass slides were cleaned in an ultrasonic bath with acetone and ethanol, respectively. Lastly they were rinsed with distilled water and dried. After the above treatment, spin coating process was applied to cover solutions on the glass substrates. Holmarc Spin Coating Unit was used for spinning process and coating was done by quickly depositing ~0.6 mL of solution onto a glass substrate spun at 6000 rpm for 30 s in air. To prepare as-deposited films, five spin coating cycles were carried out for each substrate. After each spinning cycle, samples were subjected to repeated annealing at 300 ºC for a five-minute period and finally were post-annealed at 500 ºC for one hour in oven.

X-ray diffraction (XRD) patterns of thin films have been determined by a Bruker D8 Advance X-ray diffractometer with CuK_α radiation. Besides, the morphological characterizations of the thin films have been analysed by Zeiss LS-10 atomic force electron microscope (AFM). For optical characterization, the transmittance spectra were measured from 350 nm to 1500 nm wavelength using Jasco Model V-570 type UV-Vis-NIR spectrophotometer at room temperature. Furthermore, thicknesses of thin films were measured by using Woolam Vase M2000 ellipsometer. Thicknesses increase orderly with increament in dopant concentration. These results are shown in Table 1.

3. RESULTS AND DISCUSSION

3.1. Optical Characterization

To investigate the effects of Au nanoparticles doping on the optical properties of TiO_2 thin films, transmittance spectra (T) for all films were measured and optical parameters such as, optical band gap (E_g), refractive index (n), extinction coefficient (k) were calculated. Fig. 2 shows transmittance spectra in wavelength range (300 – 1500) nm. As shown in Fig. 2 and Table 1, the transmission values of pure TiO_2 and Au NPs doped TiO_2 thin films (10 %, 20 %, 30 %, 40 % and 50 %) are 78.8 %, 87.8 %, 88.4 %, 93.3 %, 67.2 % and 58.5 %, respectively, in the 500 nm wavelenght. The increament in values for transmittance observed for pure and under 40 % dopant values by Au NPs doped TiO_2 thin films. This increase in transparency is related to the structural properties of the film characteristics, because it is known that the changes in transmittance depend on the material characteristics of the films [26]. Over 40 % values, the transmittance curves show strong damping due to high density of free electrons.

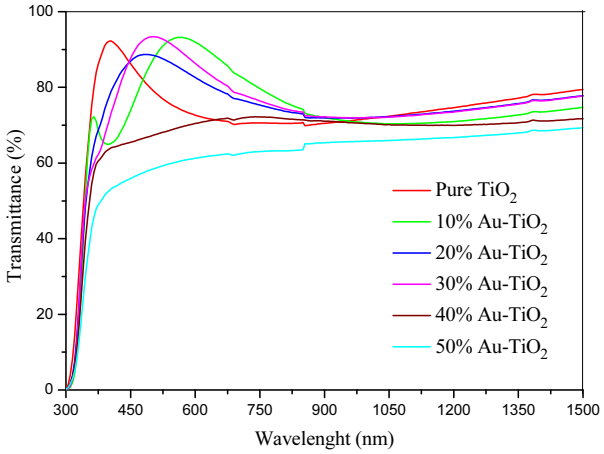

Fig. 2. Optical transmission spectra of TiO_2 thin films doped at various Au NPs concentrations

Table 1. Some optical constant of TiO_2 thin films at various Au NPs concentrations

Material	d (nm)	$T_{@\ 500\ nm}$ (%)	E_g (eV)
Pure TiO_2	132	78.8	3.74
10 % Au doped TiO_2	138	87.8	3.75
20 % Au doped TiO_2	144	88.4	3.78
30 % Au doped TiO_2	149	93.3	3.84
40 % Au doped TiO_2	154	67.2	3.86
50 % Au doped TiO_2	166	58.5	3.89

The optical band gap data of the thin films were achieved by the relation [1]:

$$(\alpha h\nu) = A(h\nu - E_g)^{1/2}. \quad (1)$$

The equation gives the band gap energy, when straight portion of $(\alpha h\nu)^2$ against hν plot is extrapolated to the point $\alpha = 0$. Figure 3 shows the relation between $(\alpha h\nu)^2$ and photon energy $h\nu$ for pure and Au NPs doped TiO_2 thin films.

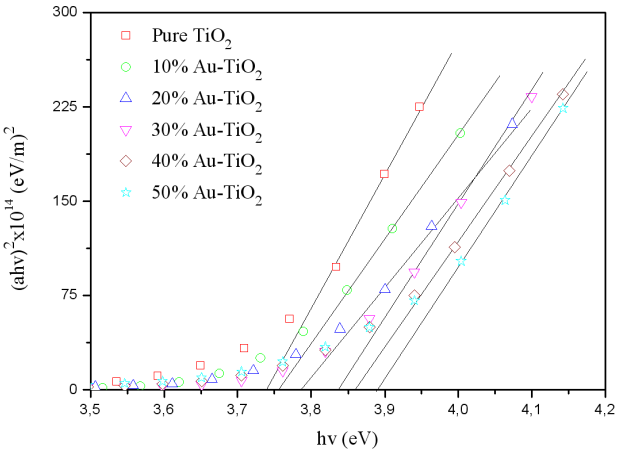

Fig. 3. $(\alpha h\nu)^2$ versus hν graph of TiO_2 thin films doped at various Au NPs concentrations

The band gap value of TiO_2 thin films increases with the increasing Au nanoparticles concentrations. The widening of the band gap can be explained by the Burstein-Moss (BM) effect [27], in which the lowest states in the conduction band were blocked, and transitions can take place only to energies higher than Fermi energy. Thus,

the band gap became widened with increasing Au nanoparticles concentrations. Also, grain growth inhibition by increasing Au nanoparticles concentrations in the films causes smaller sizes which leads to larger band gap energy [28]. A decrease of the band gap energy with the increasing in Au dopant concentration has been reported, which prepared by sol-gel method [22]. However, the doping of various transtional metal ions into TiO_2 could shift its optical absorption edge from the UV into the visible light range, but no prominent change in the TiO_2 band gap was observed [33].

The complex optical refractive index of the films is described by the following relation [29]:

$$\tilde{n} = n(\omega) + ik(\omega)\,, \tag{2}$$

where n is the real part and k is the imaginary part (extinction coefficient) of complex refractive index. The refractive index of the samples can be obtained from the following equation [30]:

$$n = \frac{1+R}{1-R} + \sqrt{\frac{4R}{(1-R)^2} - k^2}\,, \tag{3}$$

where R is the reflectance and $k = (\alpha\lambda / 4\pi)$ is the extinction coefficient. The refractive index values were calculated by using Eq. (3). The variation of the refractive index (n), the extinction coefficient (k) with wavelength for the TiO_2 thin films at different Au nanoparticles concentrations is shown in Figs. 4 and 5 respectively.

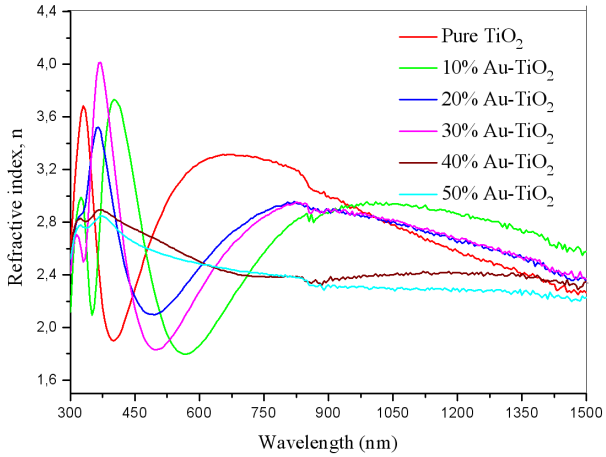

Fig. 4. The variation of refractive index of TiO_2 thin films doped at various Au NPs concentrations with wavelength

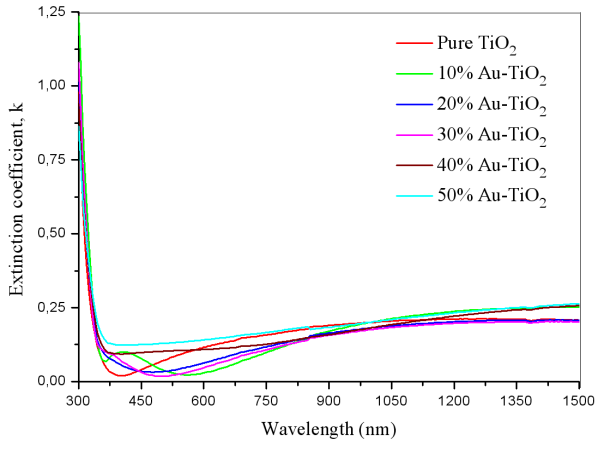

Fig. 5. The variation of extinction coefficient of TiO_2 thin films doped at various Au NPs concentrations with wavelength

As shown in Figs. 4 and 5, the values of n and k are changing with increase in λ. These observations verify the reduction in the loss of light due to scattering and absorbance with increase in wavelength.

What is the physical nature of this 'double peak' feature? The most feasible explanation would be the interaction of a portion of Au-NPs with the glass substrate, but not in the case of the extinction spectra measured in the same plasmonic layers deposited on a glass substrate. This is why we disregard the effect of either nanoparticle agglomerates or localized surface plasmon resonans (LSPR) modes associated with elongated/triangular Au-NPs. The LSPR maximum wavelength in metal NPs is very sensitive to the refractive index of their surrounding medium and hence a rough estimate of the LSPR can be based on the assumption that Au-NPs formed on the glass substrate are embedded in a medium whose dielectric constant is the arithmetic average value between those of the two materials on either side of their interface, namely the TiO_2 matrix ("titania) and glass [34 – 35].

3.2. Structural Characterization

Fig. 6 shows the XRD spectra of the pure and Au nanoparticles doped TiO_2 thin films. The pure TiO_2 thin film has the anatase phase crystal plane with (101) reflection while Au nanoparticles doped TiO_2 thin film also exhibited characteristic peaks of anatase crystal plane (101) and (200). The releative peak intensity of these diffraction peaks increases with Au NPs doping and resulted in better crystallity.

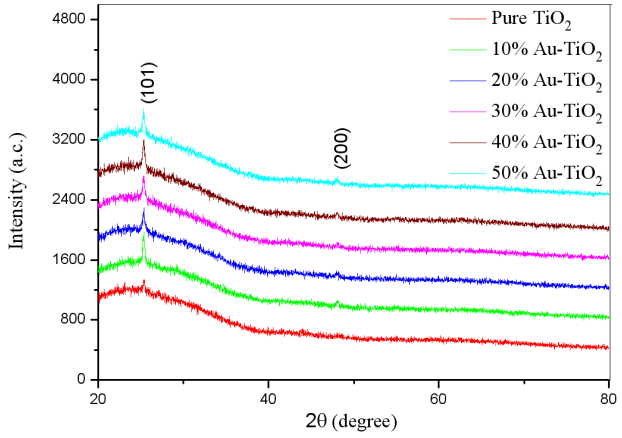

Fig. 6. X-ray diffraction pattern of TiO_2 thin films at various Au NPs concentrations

XRD is essential to determine the crystal structure and crystallinity, and to estimate the crystal size according to the Scherrer equation [31, 32]:

$$D = \frac{0.9\lambda}{\beta \cos\theta_\beta}\,, \tag{4}$$

where D is the crystallite size, 0.9 is a constant, λ is the wavelength and β is the full width at half maximum of diffraction peak measured in radians and θ is the Bragg angle. The broadening of a particular peak in a diffraction pattern associated with a particular planar reflection from within the crystal unit cell is measured to determine crystal size. The anatase crystallites sizes in pure TiO_2 and Au-doped TiO_2 thin films (10 %, 20 %, 30 %, 40 % and 50 %) are 19.87, 24.32, 25.12, 28.41, 31.55, 35.21 nm

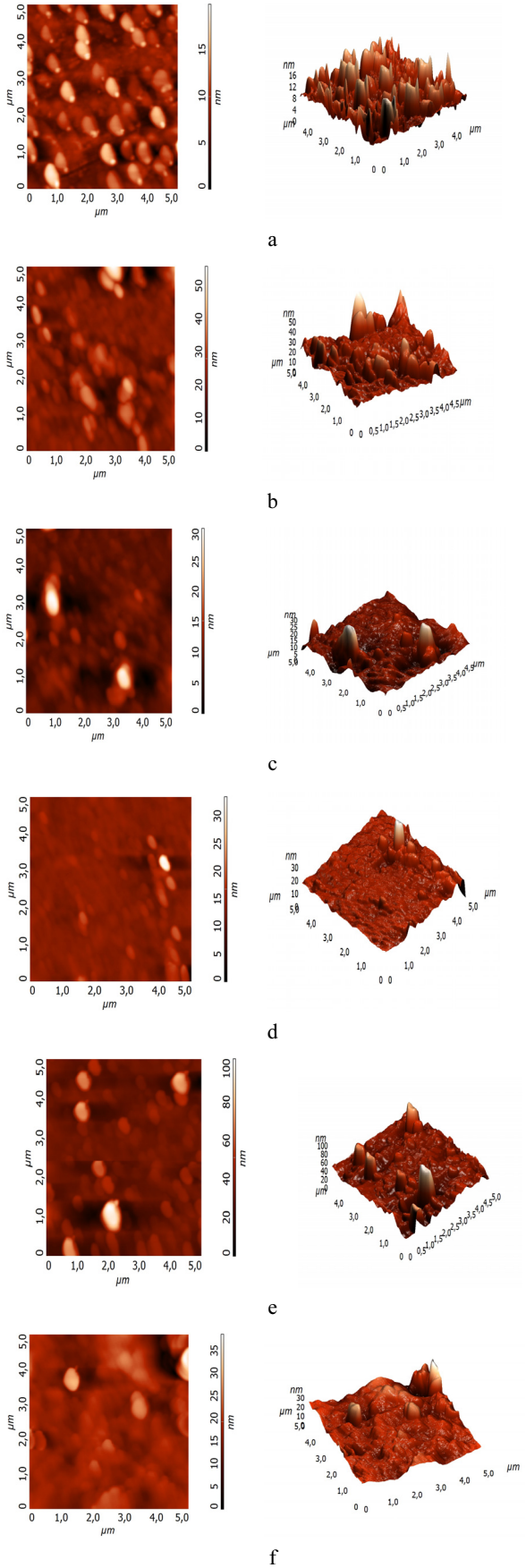

Fig. 7. AFM 2D and 3D images of: a – pure TiO_2; b – 10 % Au-doped TiO_2; c – 20 % Au-doped TiO_2; d – 30 % Au-doped TiO_2; e – 40 % Au-doped TiO_2; f – 50 % Au-doped TiO_2

respectively. The calculated values indicate that the crystallite size increases with Au-NPs doping in terms of crystal plane (101) of anatase structure. All of the thin films give similar patterns without any peak having Au NPs. Absenting of Au characteristic patterns can be explained by dispersing Au nanoparticles in the thin films uniformly. On the other hand, the presence of Au content influences the crystallite sizes. The results plotted in Fig. 6 were probably due to the crystallinity of the samples being improved. The crystallite sizes become larger with increase of Au concentration owing to increased ionic radii and atomic weight of Au^{+} as compared to Ti^{2+}. The increment is accordance with results available in the literature [22].

3.3. Morphological Characterization

Fig. 7, a – f, shows the two-dimensional (2D) and three-dimensional (3D) AFM images of the pure, 10 %, 20 %, 30 %, 40 % and 50 % Au nanoparticles-doped TiO_2 thin films, respectively.

The 2D images show that the films are uniform and the substrate surface is well covered with grains that are almost uniformly distributed over the surface. The 3D images exhibit large nicely separated conical columnar grains in all thin films. The average surface roughness and the average grain size increases from 2.21 nm to 7.63 nm and from about 167 nm to 542 nm with increase of the Au nanoparticles content. This may be due to the bigger clusters formed by the coalescence of two or more grains. [17]. Following the other work, Buso et al. prepared gold nanoparticle doped TiO_2 semiconductor thin films by using sol-gel method and found that values of the average surface roughness in the (0.3 – 0.6) nm and (0.3 – 0.8) nm ranges for TiO_2 and 8 % doping Au-TiO_2 films, respectively [36].

4. CONCLUSION

In this study, pure and Au NPs doped TiO_2 thin films were sythesized using sol-gel method and also, the effect of Au NPs doping on the optical, structural and morphological properties of these thin films was investigated. From the optical investigations, the highest values of pure and Au NPs doped TiO_2 thin films, containing under 40 % dopant values, were observed. The optical band gap of the TiO_2 thin films increases with Au NPs doping from 3.74 eV to 3.89 eV. The widening of the band gap can be explained by the Burstein-Moss (BM) effect. XRD measurements revealed that TiO_2 thin films were polycrystalline with a body-centered tetragonal structure in anatase phase and the crystallite sizes increased with Au NPs doping for all thin films. From AFM images, the average surface roughness and the average grain size increased with increase of the Au nanoparticles. This may be due to the bigger clusters formed by the coalescence of two or more grains with increasing of Au nanoparticles concentration. As a conclusion, the structural, morphological and optical properties of the TiO_2 thin films could be controlled by Au nanoparticles-doping.

REFERENCES

1. **Sönmezoğlu, S., Çankaya, G., Serin, N.** Influence of Annealing Temperature on Structural, Morphological and Optical Properties of Nanostructured TiO_2 Thin Films *Materials Technology* 27 (3) 2012: pp. 251 – 256.

2. **Mayer, J. T., Diebold, U, Madey, T. E., Garfunkel, E.** Titanium and Reduced Titania Overlayers on Titanium Dioxide (110) *Journal of Electron Spectroscopy and Related Phenomena* 7 1995: pp. 1 – 11. http://dx.doi.org/10.1016/0368-2048(94)02258-5
3. **Sönmezoğlu, S.** Processing and Electrical Characterization of Metal-Oxide-Semiconductor Structures Prepared by DBSA-Doped TiO_2 Nanoparticles *Current Nanoscience* 9 2013: pp. 39 – 45.
4. **Yoon, K.-M., Yang, K.-Y., Byeon, K.-J., Lee, H.** Enhancement of Light Extraction in GaN Based LED Structures Using TiO_2 Nano-structures *Solid-State Electronics* 54 2010: pp. 484 – 487.
5. **Sönmezoglu, S., Akyürek, C., Akın, S.** High-efficiency Dye-sensitized Solar Cells Using Ferrocene-based Electrolytes and Natural Photosensitizers *Journal of Physics: D-Applied Physics* 45 2012: pp. 425101 – 425107.
6. **Huang, L., Liu, T. M., Zhang, H. J., Guo, W. W., Zeng, W.** Hydrothermal Synthesis of Different TiO2 Nanostructures: Structure, Growth and Gas Sensor Properties *Journal of Materials Science-Materials in Electronics* 23 2012: pp. 2024 – 2029. http://dx.doi.org/10.1007/s10854-012-0697-6
7. **Zhang, M. L., Yuan, Z. H., Song, J. P., Zheng, C.** Influence of Surface States on Gas Response Properties of Pt/TiO_2 *Journal of Inorganic Materials* 27 2012: pp. 928 – 932.
8. **Kang, S. H., Lee, W., Nah, Y. C., Lee, K. S., Kim, H. S.** Synthesis of Nanobranched TiO_2 Nanotubes and Their Application to Dye-sensitized Solar Cells *Current Applied Physics* 13 (1) 2013: pp. 252 – 255.
9. **Zhong, P., Que, W., Liao, Y.** Improved Performance in Dye-sensitized Solar Cells by Rationally Tailoring Anodic TiO_2 Nanotube Length *Journal of Alloys and Compounds* 540 2012: pp. 159 – 164. http://dx.doi.org/10.1016/j.jallcom.2012.06.088
10. **Jo, W. K., Kang, H. J.** LED Irradiation of a Photocatalyst for Benzene, Toluene, Ethyl Benzene, and Xylene Decomposition *Chinese Journal of Catalysis* 33 2012: pp. 1672 – 1680.
11. **Rabaste, S., Bellessa, J., Briouride, A., Bovier, C., Plenet, J. C., Brenier, R., Marty, O., Mugnier, J., Dumas, J.** Sol-gel Fabrication of Thick Multilayers Applied to Bragg Reflectorsand Microcavities *Thin Solid Films* 416 2002: pp. 242 – 247.
12. **Lee, K. S., Lim, J. W., Kim, H. K., Alford, T. L. Jabbour, G. E.** Transparent Conductive Electrodes of Mixed TiO_2-x-indium Tin Oxide for Organic Photovoltaics *Applied Physics Letters* 100 2012. DOI: 10.1063/1.4707381.
13. **Chung, S. M., Shin, J. H., Hong, C. H., Cheong, W. S.** Thin Film Transistor Based on TiO_x Prepared by DC Magnetron Sputtering *Journal of Nanoscience and Nanotechnology* 12 2012: pp. 5440 – 5443. http://dx.doi.org/10.1166/jnn.2012.6228
14. **Akın, S., Sönmezoğlu, S.** Nanostructured TiO_2 Thin Films: Synthesis and Characterisations *Materials Technology: Advanced Performance Materials* 27 2012: pp. 342 – 349.
15. **Sönmezoğlu, S.** Current Transport Mechanism of p–ZnO/ /n–TiO_2 Heterojunction Diode *Applied Physics Express* 4 2011: pp. 104104 – 104106. http://dx.doi.org/10.1143/APEX.4.104104
16. **Sönmezoğlu, S., Arslan, A., Serin, T., Serin, N.** The Effects of Film Thickness on the Optical Properties of TiO_2-SnO_2 Compound Thin Films *Physica Scripta* 84 2011: pp. 065602 – 065607.
17. **Sönmezoğlu, S., Çankaya, G., Serin, N.** Phase Transformation of Nanostructured Titanium Dioxide Thin Films Grown by Sol-gel Method *Applied Physics A: Materials Science & Processing* 107 2012: pp. 233 – 241. http://dx.doi.org/10.1007/s00339-011-6749-6
18. **Mitsuhara, K., Kitsudo, Y., Matsumoto, H.** Electronic Charge Transfer Between Au Nano-particles and TiO_2-terminated $SrTiO_3$(0 0 1) Substrate *Surface Science* 604 2010: pp. 548 – 554. http://dx.doi.org/10.1016/j.susc.2009.12.024
19. **Loganathan, K., Bommusamy, P., Muthaiahpillai, P., Velayutham, M.** The Syntheses, Characterizations, and Photocatalytic Activities of Silver, Platinum, and Gold Doped TiO_2 Nanoparticles *Environmental Engineering Research* 16 2011: pp. 81 – 90.
20. **Eremenko, A., Gnatiuk, I., Linnik, O., Vityuk, N., Mukha, I., Korduban, A.** Silver and Gold Nanoparticles on Sol-gel TiO_2, ZrO_2, SiO_2 Surfaces *Nanocomposites and Polymers with Analytical Methods* 3 2011: pp. 52 – 81.
21. **Torres, D. T., Valdez, M. T., Castaneda, L., Torres, C. T., Rivera, L. T., Fernandez-Hernandez, R. C. Reyes-Esqueda, J. A., Muñoz-Saldaña, J., Rangel-Rojo, R., Oliver, A.** Inhibition of the Two-photon Absorption Response Exhibited by a Bilayer TiO_2 Film with Embedded Au Nanoparticles, *Optics Express* 18 2010: pp. 16406 – 16417. http://dx.doi.org/10.1364/OE.18.016406
22. **Rahulan, K. M., Ganesan, S., Aruna, P.** Synthesis and Optical Limiting Studies of Au-doped TiO_2 Nanoparticles *Advances in Natural Sciences: Nanoscience and Nanotechnology* 2 2011: pp. 025012 – 025017.
23. **Yu, K., Tianw, Y. Tatsuma, T.** Size Effects of Gold Nanoparticles on Plasmon-induced Photocurrents of Gold-TiO_2 Nanocomposites *Physical Chemistry Chemical Physics* 8 2006: pp. 5417 – 5420. http://dx.doi.org/10.1039/b610720f
24. **Brust, M., Bethell, D., Kiely, C. J., Schiffen, D. J.** Self-assembled Gold Nanoparticle Thin Films with Nonmetallic Optical and Electronic Properties *Langmuir* 14 1998: pp. 5425 – 5429.
25. **Gultekin, A., Ersöz, A., Hür, D., Sarıözlü, N. Y., Denizli, A., Say, R.** Gold Nanoparticles Having Dipicolinic Acid Imprinted Nanoshell for Bacillus cereus Spores Recognition *Applied Surface Science* 256 2009: pp. 142 – 148. http://dx.doi.org/10.1016/j.apsusc.2009.07.07
26. **DeNeufville, J. P., Moss, S. C., Ovshinsky, S. R.** Photostructural Transformations in Amorphous As_2Se_3 and As_2S_3 Films *Journal of Non-crystalline Solids* 13 1973: pp. 191 – 223. http://dx.doi.org/10.1016/0022-3093(74)90091-X
27. **Yang, Y., Chen, X., Feng, Y., Yang, G.** Physical Mechanism of Blue-Shift of UV Luminescence of a Single Pencil-like ZnO Nanowire *Nano Lett*ers 12 2007: pp. 3879 – 3883. http://dx.doi.org/10.1021/nl071849h
28. **Brus, L.** Electronic Wave-functions in Semiconductor Clusters. Experiment and Theory *Journal of Physical Chemistry* 90 1986: pp. 2555 – 2560. http://dx.doi.org/10.1021/j100403a003
29. **Wolaton, A. K, Moss, T. S.** Determination of Refractive Index and Correction to Effective Electron Mass in PbTe and PbSe *Proceeding of the Royal Society B* 81 1963: pp. 509 – 513.
30. **Bass, M., Cusatis, C. D., Enoch, J., Li, G., Mahajan, V. N., Lakshminarayanan, V., Stryland, E. V., MacDonald, C.** Handbook of Optics: Optical Properties of Materials, Nonlinear Optics, Quantum Optics. Chicago: McGraw-Hill, 2009.
31. **Cullity, B. D., Stock, S. R.** Elements of X-ray Diffraction. New Jersey, Prentice-Hall, Englewood Cliffs, 2001.
32. **Scherrer, P.** Bestimmung der Grösse und der Inneren Struktur von Kolloidteilchen Mittels Röntgenstrahlen, Nachrichten von der Gesellschaft der Wissenschaften, Göttingen *Mathematisch-Physikalische Klasse* 2 1918: pp. 98 – 100.
33. **Wu, J. C. S., Chen, C. H.** A Visible-light Response Vanadium-doped Titania Nanocatalyst by Sol-gel Method *Journal of Photochemistry Photobiology* 163 2004: pp. 509 – 515.
34. **Palik, E, D.** (ed). Handbook of Optical Constants of Solids. San Diego: Academic Press, 1998, 529 p.
35. **Tanabe, I., Tatsuma, T.** Plasmonic Manipulation of Color and Morphology of Single Silver Nanospheres *Nano Lett*ers 12 2012: pp. 5418 – 5421.
36. **Buso, D., Pacifico, J., Martucci, A., Mulvaney, P.** Gold-nanoparticle-doped TiO_2 Semiconductor Thin Films: Optical Characerization *Advanced Functional Materials* 17 2007: pp. 347 – 354. http://dx.doi.org/10.1002/adfm.200600349